



## EXPERIMENTAL MEASUREMENTS ON A CIRCULAR DISC IN FLOW

Khalid A. Joudi      Abdullah A. Kendoush      Abdul-Rahman J. Mohammed  
Department of Mechanical Engineering University of Baghdad, Baghdad-Iraq

### ABSTRACT

An experimental investigation was made for the study of incompressible flow on a circular disc. It consists of two parts. The first was the determination of the pressure distribution of the front and rear sides of three samples of discs with diameters 9.73, 10.75 and 11.94 cm and 3 mm thickness. The discs were mounted normal to the flow direction. This part also included the determination of pressure distribution on the front and rear sides of an inclined disc of 10.75 cm diameter at inclination angles of 30°, 60°, 120°, and 150° to the horizontal. The second part of the investigation was the determination of the drag coefficient on a circular disc 10.75 cm in diameter and 3 mm in thickness using two methods. The first using strain gages as sensitive elements. The strain readings were recorded and transformed into drag force by using a transformation system or by using the strain transformation equations. The second using a dial gage whereby the displacement was transformed into drag force. Drag determination was performed for normal and inclined discs. Inclination included 30°, 60° and 90° to the horizontal. Tests were made using a low speed wind tunnel, at low, medium and high velocities of 4.74, 8.316 and 10.35 m/s respectively. The experimental results compared well with theoretical predications and with available published data.

### الخلاصة

تم في هذا البحث إنجاز دراسة مختبرية للجريان المنتظم اللانضغاطي على قرص دائري، تضمنت الدراسة جريانين حيث تضمن الجزء الأول قياس توزيع الضغط على السطح الامامي والسطح الخلفي لثلاثة نماذج من الأقراص الدائرية ذات الأقطار 9,73 و 10,75 و 11,94 سم وبسمك 3 ملم لكل منها وكانت زاوية ميلان القرص عن المحور الأفقي 90 درجة. كما تم حساب توزيع الضغط على السطحين الامامي والخلفي لقرص دائري ذي قطر 10,75 سم ولكن بزوايا ميل مختلفة هي 30 و 60 و 120 و 150 درجة على التوالي. أما الجزء الثاني من الدراسة فتضمن حساب معامل السحب من خلال حساب قوة السحب على قرص دائري ذو قطر 10,75 سم وبسمك 3 ملم بطريقتين. الطريقة الأولى هي طريقة استخدام مقياس الانفعال كمتحسسات ويتم تسجيل القراءات ثم تحويل هذه القراءات إلى قوة السحب عن طريق استخدام نظام تحويل أو عن طريق استخدام معادلات الانفعال ومنها يستخرج معامل السحب. أما الطريقة الثانية فكانت باستخدام جهاز مقياس الأزايا و تحويلها إلى قوى باستخدام نظام تحويل الأزايا إلى قوة وبالتالي معامل السحب. وقد أجريت التجارب لثلاث زوايا هي 30، 60، 90 بالدرجات.



تم إجراء التجارب في نفق هوائي ذو ثلاث سرع هي ٤,٧٤ و ٨,٣١٦ و ١١,٩٤ م/ثا وتمت مقارنة نتائج توزيع الضغط مع معادلات نظريه وكان التوافق جيدا.

## KEYWORDS

Fluid mechanics, flow on a disc, drag coefficient and pressure distribution on a disc facing uniform flow.

## INTRODUCTION

Recently several aerospace oriented engineering problems have arisen which have prompted renewed interest in disc aerodynamics. One such example is the uncertainty introduced by aerodynamically induced oscillations of balloons used to measure the vertical profile of atmospheric winds. In addition, the lack of understanding of bluff-body flows stimulates further study. Some studies were conducted for calculating the drag and pressure distribution on bluff bodies using different methods. Some were theoretical like studies for the steady motion of a disc conducted by Michael (1966) who solved the Navier-Stokes equation by numerical iteration and determined the drag coefficient. Another was conducted by Kendoush (2000) to find the pressure distribution for the front and rear sides of the disc. While other studies tried to find the drag and pressure distribution experimentally. An example is the experimental investigation of a disc moving rectilinearly through incompressible fluid conducted by Ross and Willmarth (1971) to find the drag coefficient of that disc. Another experimental study was conducted by Calvert (1967) who used a wind tunnel to perform experiments on a disc at different angles of incidence to measure the drag coefficient  $C_D$  and the pressure distribution on a circular disc.

## EXPERIMENTAL EQUIPMENT

### The System Layout for Pressure Distribution Measurement

Three sizes of discs of diameters 9.73, 10.7 and 11.97 cm were made and tested. The experiments were performed on the circular disc facing uniform flow. The discs were all of 3-mm thickness. The discs were fixed externally at the exit of the wind tunnel by a supporting system of rigid material, to prevent the effect of deflection on the model as shown in Fig. (1). A system of screws is used to connect the disc with the arm and can change its angle of incidence.

An important point is that any strut or wire connecting the model causes extraneous forces, which influence the reading of the instrument. One effect is the drag of the exposed strut or wire. Another is the presence of connecting tubes and holding mechanism in the free airflow. These quantities are usually lumped together and termed the interference effect. Calvert (1967), said that the interface effect of the holding and support system can be thought small and its effect is similar to that of blockage.

Circular holes were drilled along the radius of the disc. The pressure holes were arranged radially on one line along the radius of the disc as shown in Fig. (1). The diameter of the pressure holes are 2 mm through disc thickness of 3 mm so that the ratio  $L/d$  does not exceed 1.5. Ower and Pankhurst (1977), state that the error of measuring the pressure in the hole increases with the value of ratio  $L/d$  up to a value of 1.5. The distances between center to center of each hole is dependent on the diameter of the disc and their values were recorded.

The pressure of each probe hole is measured by connecting that hole to a micromanometer by rubber tubing. The other pressure holes being closed by adhesive tape to prevent the flow of air through these holes.



### Strain gage method.

A strain gage of  $120 \pm 0.5$  ohm resistance and 6mm length was mounted on the stings as shown in **Fig. (2)**. The strain gage has a  $1.76 \pm 1\%$  gage factor which represents the ratio between the change of the strain gage resistance and the change of strain gage length (Khedher, 2000). When the value of this factor increases the accuracy of strain reading will increase. The strain gage is considered as a passive transducer, which transforms the mechanical displacement into a variation of electrical resistance. It is made out of small radius wire derived from Constantine alloy, which consists of 60% copper and 40% nickel. The wire resistance varies due to variation of its length caused by the compression or tension applied, and is measured by a Wheatstone Bridge in which the strain gages are connected to the power supply of a known voltage. The output voltages are related to the strain gage resistance change. A strain gage meter of 10 channels and 4 junctions was employed. Three values of strain gage resistance 60, 120, 350 ohm were used to measure the strain.

The previous arrangement of the strain gage is mounted on the Perspex disc of 10.7cm diameter, which has smooth surface, and thickness of 3 mm. The wind tunnel is used in these experiments and two plates fixed together by a metal frame as shown in **Fig. (2)**. Two strain gages were fixed in one line of the two sides of the sting. The sting was made of aluminum and its weight can be neglected when measuring the effective forces (Khedher, 2000). The disc is supported on a steel beam, which is connected to the aluminum stings. The dimensions of stings are selected to give small deflection. The sting second moment of area about Z axis ( $I_z$ ) is  $I_z = bh^3/12$  and Young's modulus of elasticity is  $E = 70 \times 10^9$  N/m<sup>2</sup>. The sensors were set on the sting in the two defined places, as shown in **Fig. (2)**. From this system, the disc can be placed at any inclination and the forces acting on it can be measured easily.

### Dial gage method

The disc is mounted normally on the steel arm. The arm is carried by two smooth rollers, which reduce the friction force between these parts as show in **Fig. (3)**.

The steel arm is connected with the dial gage horizontally so that the displacement of the dial gage is measured in a horizontal direction which represents the drag force on the disc. The gage has 0.01mm accuracy and 25 mm total displacement. All parts are connected in one line in the direction of flow as shown in **Fig. (3)**.

The connection between the dial gage the steel arms can be represented as a point contact. This contact reduces the error coming from transforming of the moments and from forces acting on the disc except the horizontal force to the dial gage.

## RESULTS

### Pressure Distribution Profile

The results of the pressure distribution experiments are shown in **Table (1)** and **Fig. (4)**. The dimensionless pressure distribution decreases with the increase in the dimensionless radial coordinate due to the decreasing of pressure from the center of the disc to the edge, so that the pressure at the edge represents the smallest value. The reason, which made the pressure at the center of the disc,  $P_1$  larger than the pressure at the second pressure hole  $P_2$  is that when the flow of air impacts the front face of the disc, the value of the pressure  $P_1$  is approximately equal to the total pressure that is measured by the Pitot-static tube as shown in **Fig. (1)**.

In the second pressure hole the flow was not exactly normal to that point because of the divergence of the flow in the center of the disc (Davies and Taylor, 1949). In this position the direction of air can be divided into two components normal and parallel directions. The two components of velocities will impact at the second pressure hole and that will cause turbulence so that the pressure in the second probe will be smaller than the total pressure, then  $P_1 > P_2$ . In the same manner  $P_1 > P_2 > P_3 > P_4 > P_5$ . **Fig. (4)** shows that the values of rear pressure on the disc are larger than the



front side as the radial coordinate increases because of the values of pressure at the rear side are smaller than at the front side. The experimental results for pressure distribution of a disc mounted normal to the flow can be compared with the theoretical results obtained by Kendoush (2000) as shown in Figs. (5, 6) and (7) which represent curves for front side of a disc at three velocities; low, medium and high, the agreement is fair. Figs (8, 9) and (10) represent comparison of the measurements for the rear side of the disc. There is no close agreement here due to the uncertainty of the measurements.

### Effect of Inclination on Pressure and Drag Coefficient

The results for the pressure distribution on discs inclined by angles less than  $90^\circ$  are tabulated in Table (2). The results are also shown in Fig. (11). It is clear that the dimensionless pressure distribution is negative always for the front region of that disc because the pressure will decrease from the leading edge to the trailing edge. The reason is that when the disc is inclined, the front stagnation point is displaced towards the leading edge Calvert (1967). Then the dimensionless pressure distribution is always positive for the rear region which means that the pressure will increase from the leading edge to the trailing edge. The reason is that when the disc is inclined, the stagnation point is displaced towards the trailing edge, on the rear surface

The results from a disc inclined by angles more than  $90^\circ$  are tabulated in Table (3) and plotted versus the radial coordinate  $r/a$  in Fig. (12). The difference between Fig. (11) and Fig. (12) is that the dimensionless pressure distribution for front side of the disc is always positive, but the dimensionless pressure distribution for rear side of the disc is always negative. The reason was presented by Calvert (1967) as mentioned previously

Therefore, results of the drag coefficient for a disc inclined by angles of inclination  $30^\circ$ ,  $60^\circ$  and  $90^\circ$  can be plotted as the drag coefficient  $C_D$  versus  $Re$  as shown in Fig. (13). The drag coefficient  $C_D$  for normal disc was more than that for inclined disc. Then the drag coefficient values decrease as the angle of inclination decreases from  $90^\circ$ .

### CONCLUSIONS

Though many questions regarding bluff-body flows remain to be answered, the series of disc flows studies reported here has produced new information to assist in the understanding of these flows. Specific conclusions resulting from this work are:

- 1-The pressure values, measured at the center of disc represent the total pressure (impact pressure), while the pressures measured at the outer pressure holes are progressively lower.
- 2-The pressure difference values ( $P-P_C$ ) for front side was smaller than that of rear side of a disc mounted normal to the flow.
- 3-The shape of pressure distribution profile on front and rear side of disc was not affected by the size of disc.
- 4-For inclined disc when  $\theta < 90^\circ$  the pressure distribution was negative for front side and positive for rear side, but when  $\theta > 90^\circ$  the pressure distribution was positive for front side and negative for rear side
- 5-When the disc inclined by an angle more or less than  $90^\circ$  the drag force and then the drag coefficient will decrease because of the projection area will be decrease.



Table (1) Pressure Distribution on a Disc

Disc diameter (2a): 9.73 cm : Disc inclined angle ( $\theta$ ): 90°			
Center to center distance of disc between pressure probes(C): 1.1 cm			
Disc radial distance from center(r)=C* N			
N = number of pressure probes-1 : Ambient temperature (t):26°C			
Low speed = 4.74 m/s			
Density ( $\rho$ ) = 1.18kg/m <sup>3</sup>			
Number of probe	r/a	$(P-P_c/0.5 \rho V^2)_f$	$(P-P_c/0.5 \rho V^2)_R$
1	0	0	0
2	0.226	-0.0153	-0.0077
3	0.452	-0.0461	-0.01538
4	0.678	-0.1077	-0.0307
5	0.904	-0.338	-0.04615
Medium speed = 8.316 m/s			
Number of probe	r/a	$(P-P_c/0.5 \rho V^2)_f$	$(P-P_c/0.5 \rho V^2)_R$
1	0	0	0
2	0.226	-0.005	-0.01
3	0.452	-0.075	-0.015
4	0.678	-0.15	-0.02
5	0.904	-0.375	-0.025
High speed = 10.35 m/s			
Number of probe	r/a	$(P-P_c/0.5 \rho V^2)_f$	$(P-P_c/0.5 \rho V^2)_R$
1	0	0	0
2	0.226	-0.0161	-0.0483
3	0.452	-0.0645	-0.0806
4	0.678	-0.161	-0.0854
5	0.904	-0.371	-0.1



Table (2) Pressure Distribution on a Disc

Disc diameter (a): 10.75 cm : Disc inclined angle ( $\theta$ ): $60^\circ$			
Center to center distance of disc between pressure probes(C): 1.2 cm			
Disc radial distance from center (r) = C* N			
N = number of pressure probes-1 : Ambient temperature (t): $26^\circ\text{C}$			
Low speed = 4.74 m/s			
Density ( $\rho$ ): $1.18 \text{ kg/m}^3$			
Number of probe	r/a	$(P-P_c/0.5 \rho V^2)_f$	$(P-P_c/0.5 \rho V^2)_R$
1	0	0	0
2	0.223	-0.0064	0.0014
3	0.446	-0.0187	0.00287
4	0.67	-0.031	0.00575
5	0.893	-0.033	0.0107
Medium speed = 8.316 m/s			
Number of probe	r/a	$(P-P_c/0.5 \rho V^2)_f$	$(P-P_c/0.5 \rho V^2)_R$
1	0	0	0
2	0.223	-0.007	0.0007
3	0.446	-0.023	0.00116
4	0.67	-0.032	0.0084
5	0.893	-0.037	0.013
High speed = 10.35 m/s			
Number of probe	r/a	$(P-P_c/0.5 \rho V^2)_f$	$(P-P_c/0.5 \rho V^2)_R$
1	0	0	0
2	0.223	-0.042	0.00226
3	0.446	-0.025	0.00301
4	0.67	-0.034	0.0075
5	0.893	-0.042	0.015



Table (3) Pressure Distribution on a Disc

Disc diameter (2a): 10.75 cm : Disc inclined angle ( $\theta$ ): 120°			
Center to center distance of disc between pressure probes(C): 1.2 cm			
Disc radial distance from center (r) = C * N			
N = number of pressure probes-1 : Ambient temperature (t):26°C			
Low speed = 4.74 m/s			
Density ( $\rho$ ): 1.18 kg/m <sup>3</sup>			
Number of probe	r/a	$(P-P_c/0.5 \rho V^2)_f$	$(P-P_c/0.5 \rho V^2)_R$
1	0	0	0
2	0.223	0.0093	-0.00143
3	0.446	0.0147	-0.00225
4	0.67	0.0201	-0.0043
5	0.893	0.0215	-0.0057
Medium speed = 8.316 m/s			
Number of probe	r/a	$(P-P_c/0.5 \rho V^2)_f$	$(P-P_c/0.5 \rho V^2)_R$
1	0	0	0
2	0.223	0.00934	-0.0011
3	0.446	0.0163	-0.0023
4	0.67	0.0231	-0.00325
5	0.893	0.032	-0.0128
High speed = 10.35 m/s			
Number of probe	r/a	$(P-P_c/0.5 \rho V^2)_f$	$(P-P_c/0.5 \rho V^2)_R$
1	0	0	0
2	0.223	0.0105	-0.0025
3	0.446	0.0181	-0.0045
4	0.67	0.024	-0.00603
5	0.893	0.027	-0.00904



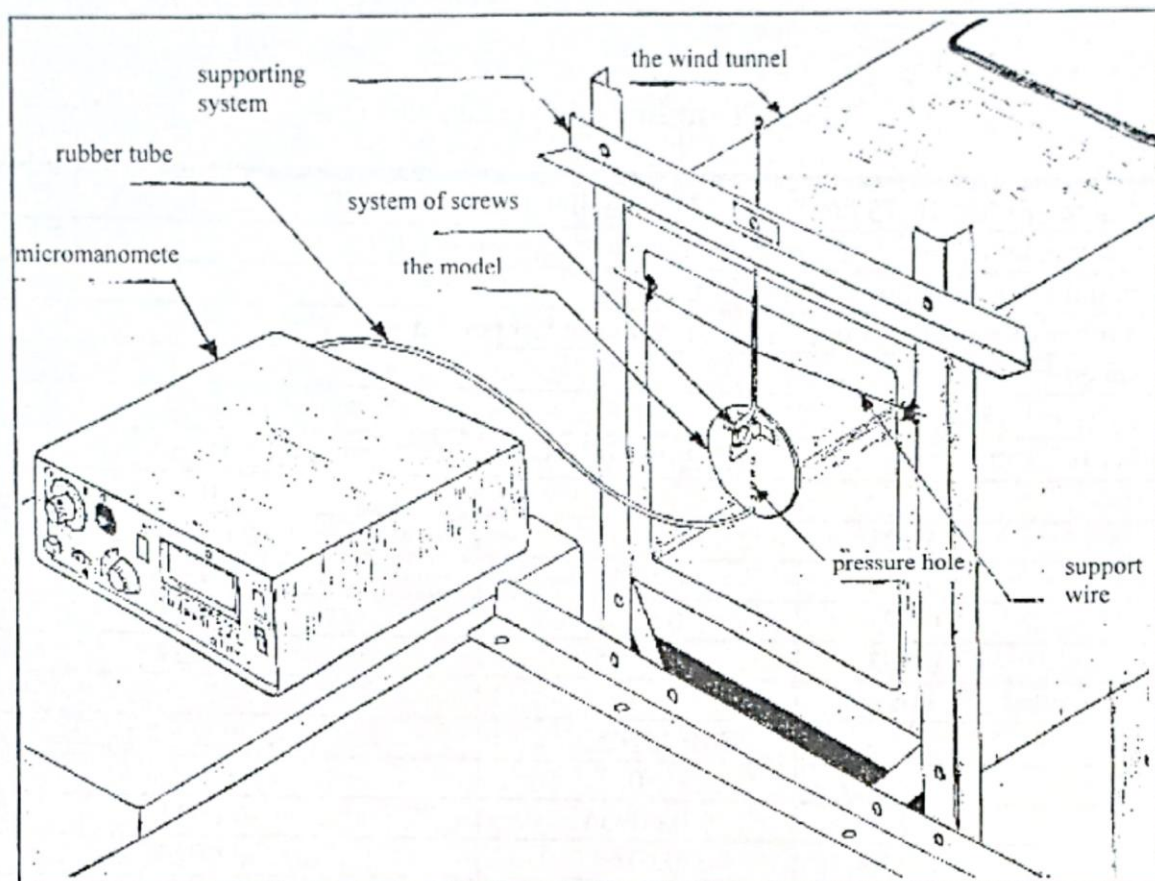


Fig. (1) Rig layout for pressure distribution measurement

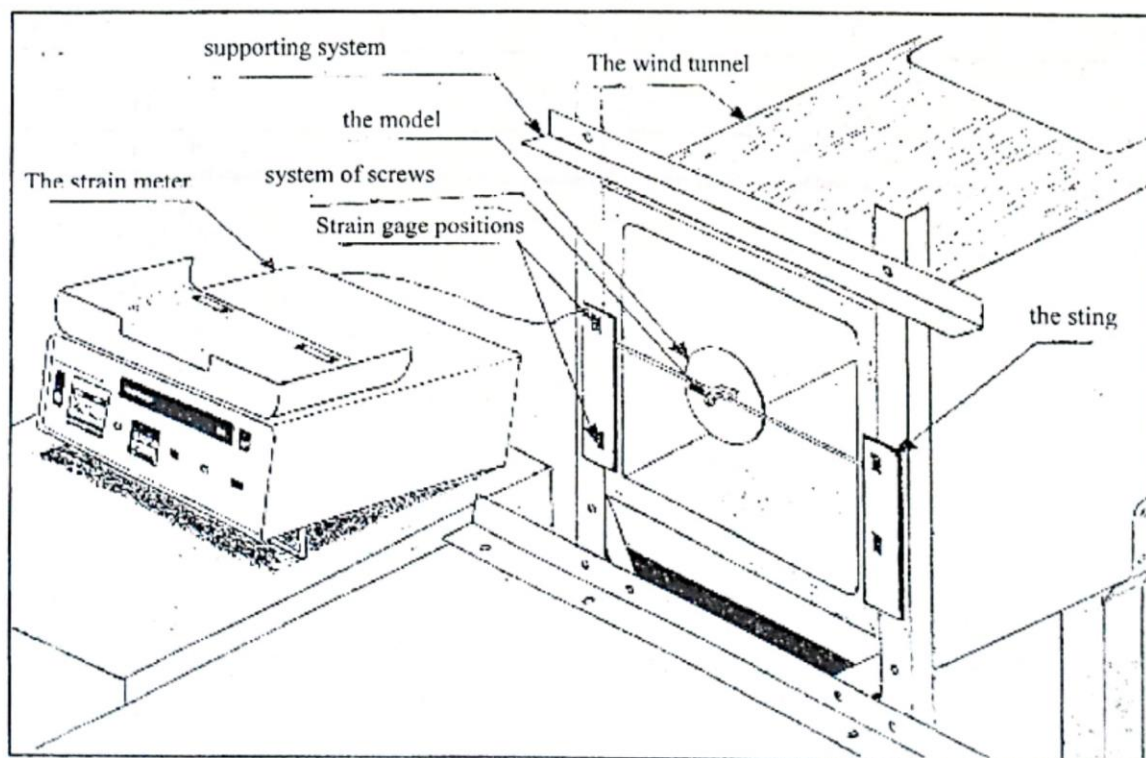


Fig. (2) Rig layout for drag measurement (strain gage method)



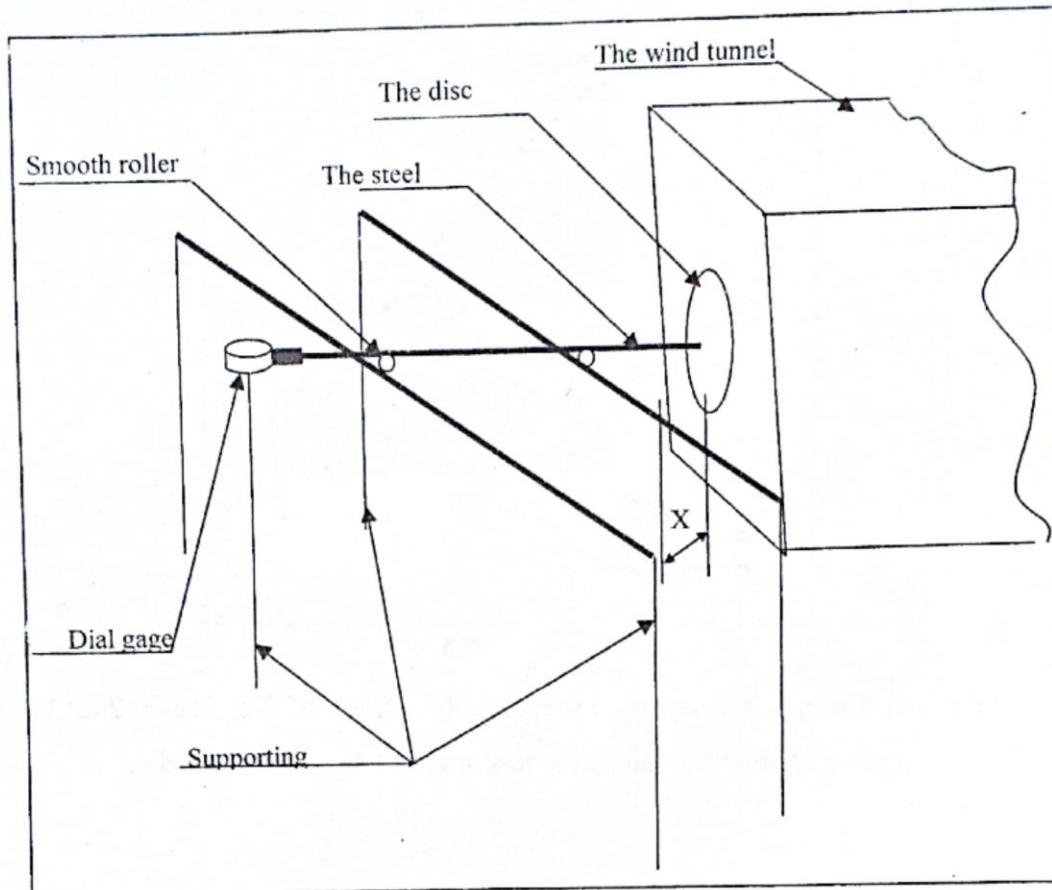


Fig.(3) Structure used to measure the drag force (Dial gage method)

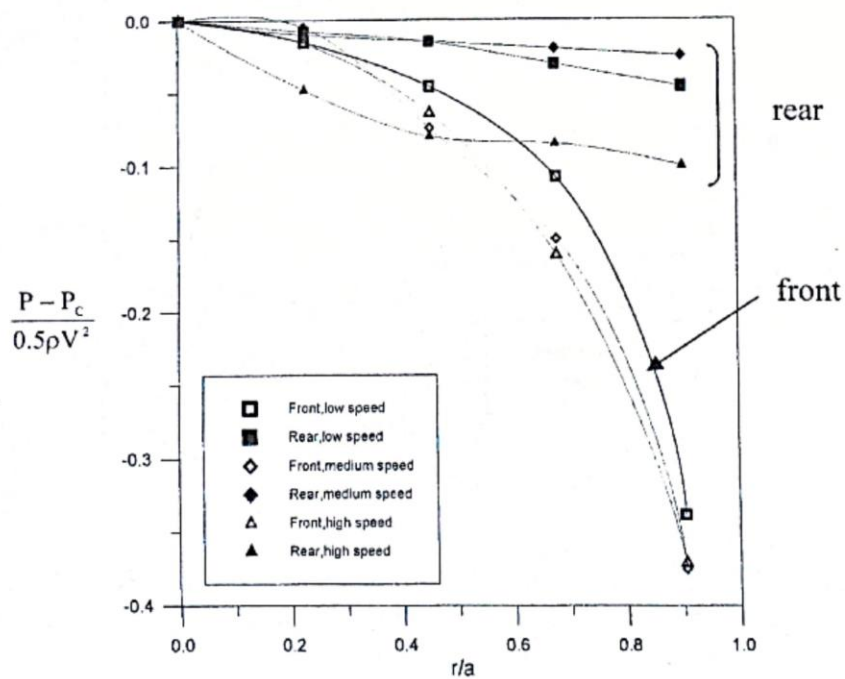


Fig. (4) Pressure distribution on the front and rear sides of disc  $T=26^\circ\text{C}$  :  $a=4.865\text{ cm}$  :  $C=1.1\text{ cm}$  :  $\theta=90^\circ$



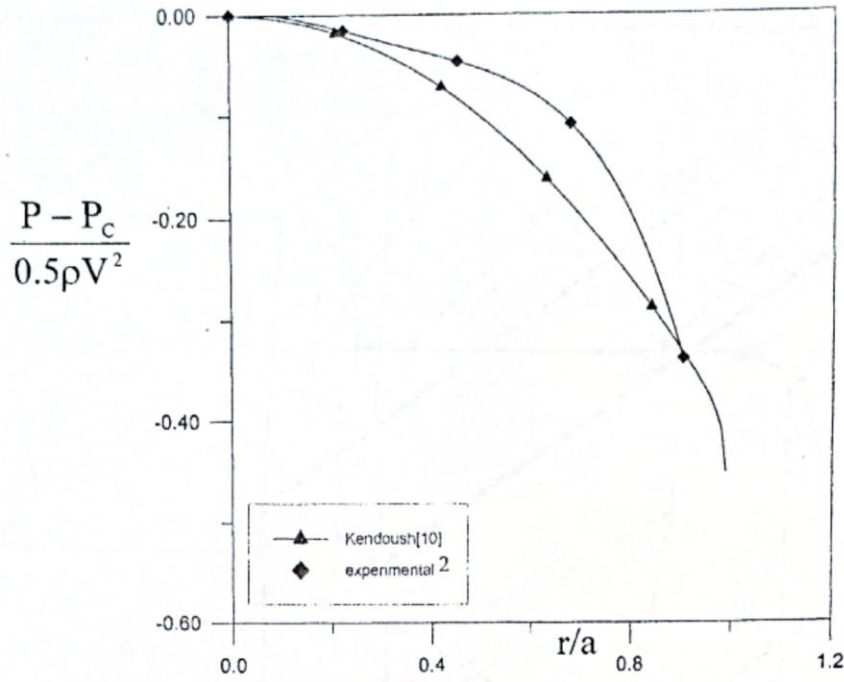


Fig. (5). Comparison between theoretical equation of Kendoush (2000) and experimental values for low speed at front side of a disc

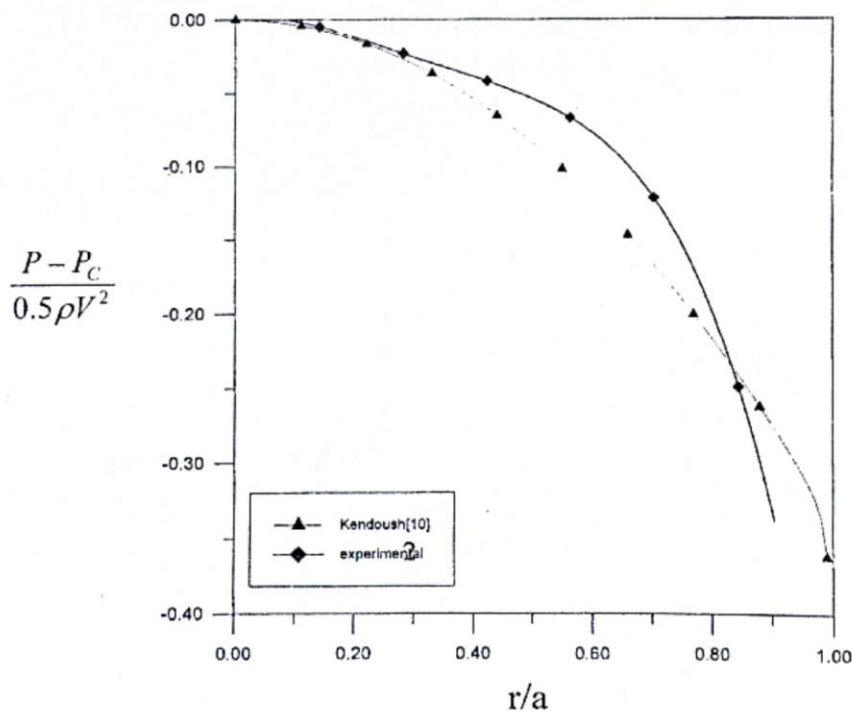


Fig. (6). Comparison between theoretical equation of Kendoush (2000) and experimental values for high speed at front side of a disc



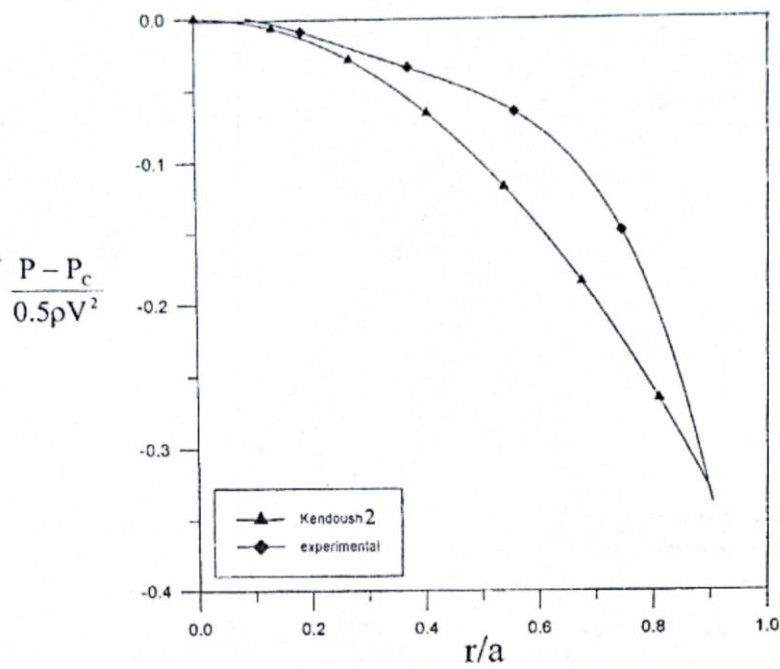


Fig. (7). Comparison between theoretical equation of Kendoush (2000) and experimental values for high speed at front side of a disc

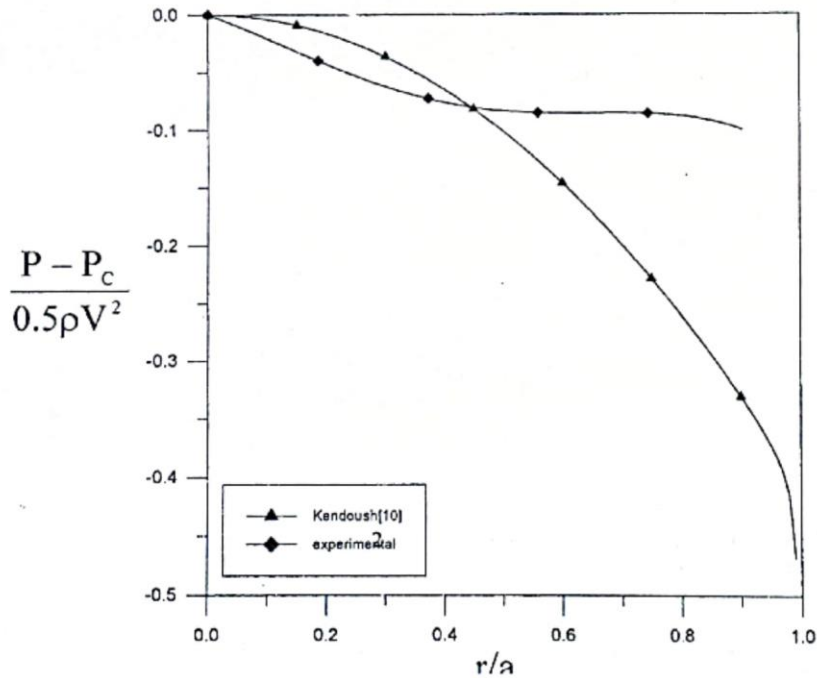


Fig. (8). Comparison between theoretical equation of Kendoush (2000) and experimental values for medium speed at rear side of a disc



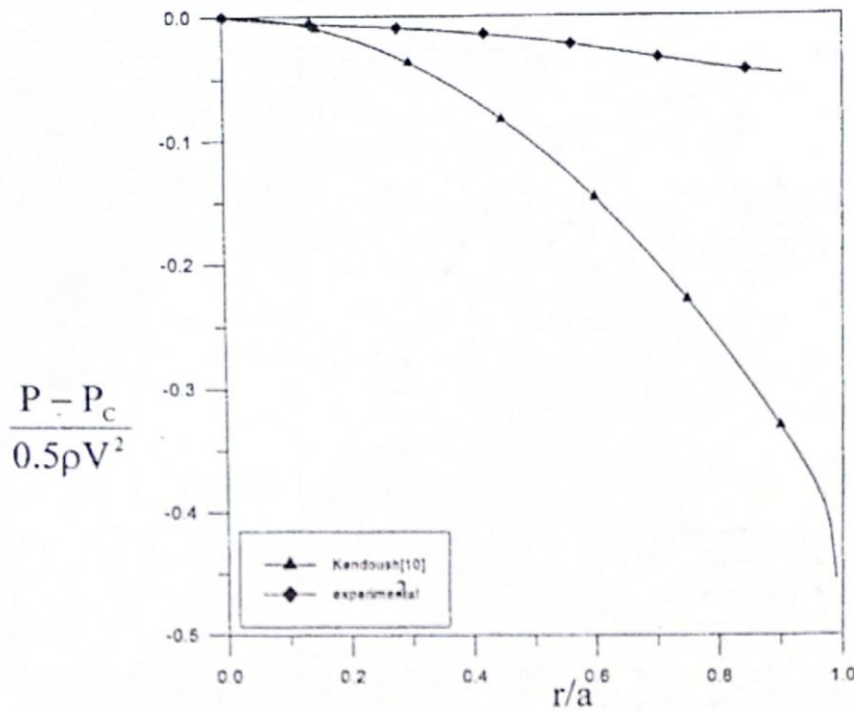


Fig. (9) Comparison between theoretical equation of Kendoush (2000) and experimental values for high speed at rear side of a disc

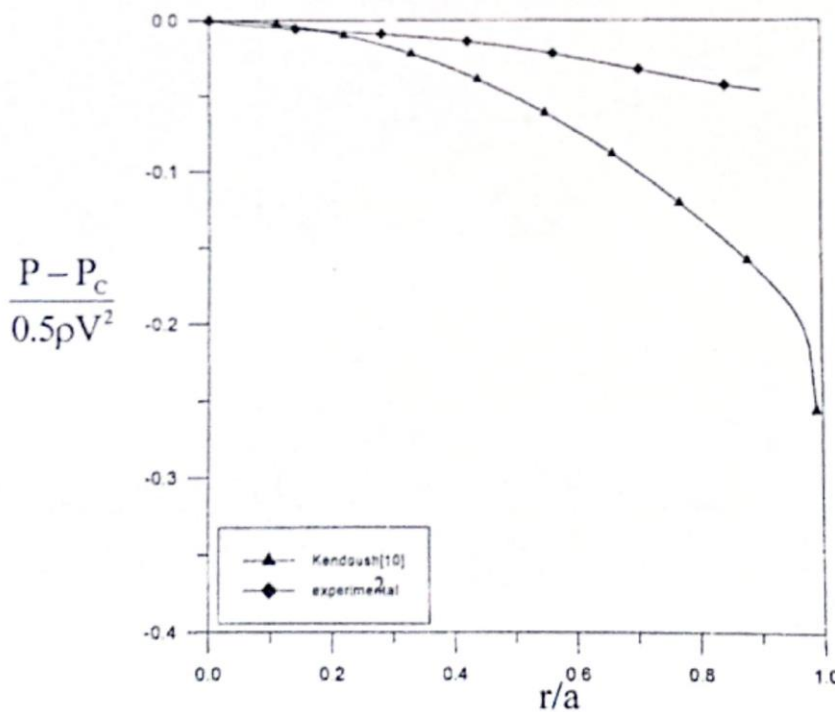


Fig. (10). Comparison between theoretical equation of Kendoush (2000) and experimental values for low speed at rear side of a disc



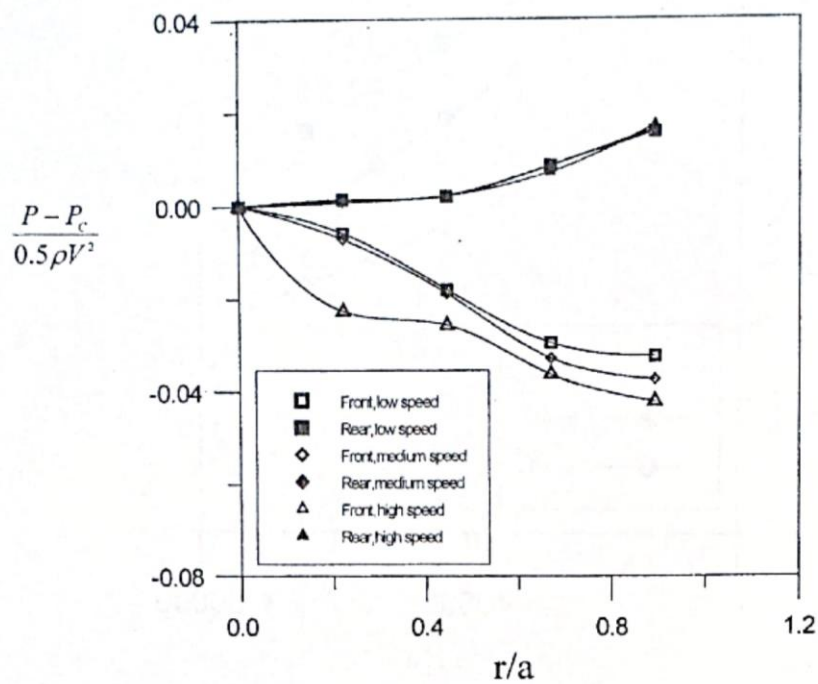


Fig. (11) Pressure distribution on the front and rear sides of disc  $T=26^\circ\text{C}$ :  $a=5.375\text{ cm}$ :  $C=1.2\text{ cm}$ :  $\theta < 90^\circ$

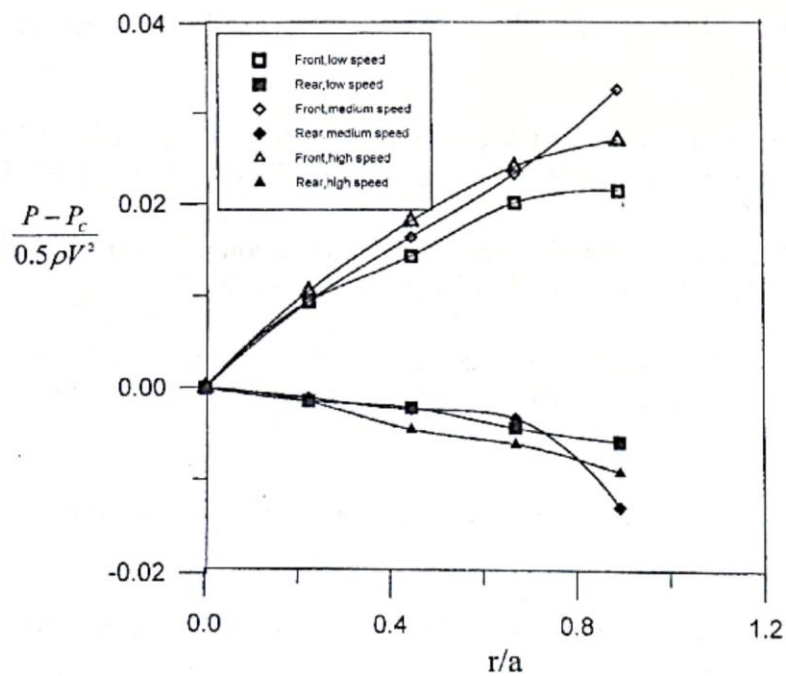


Fig. (12). Pressure distribution on the front and rear sides of disc  $T=26^\circ\text{C}$ :  $a=5.375\text{ cm}$ :  $C=1.2\text{ cm}$ :  $\theta > 90^\circ$

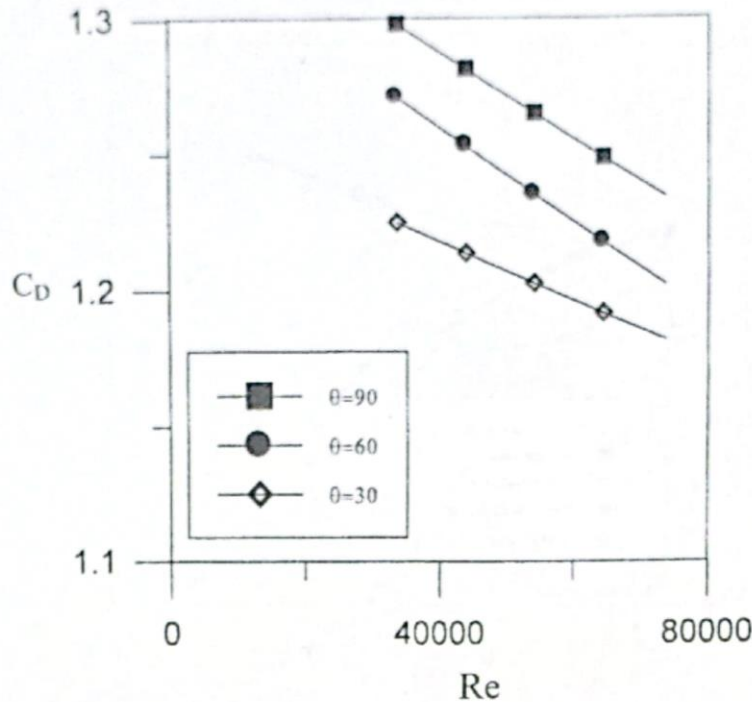


Fig. (13) The relation between  $C_D$  and  $Re$  for three different angles of inclination of disc(direct strain)

## REFERENCES

- Calvert, J.R., (1967), Experiments on the Flow Past an Inclined Disc, *Journal of Fluid Mechanics*, Vol.29, Part 4, pp 691-703.
- Davies, M., and Taylor, G., (1949), The Mechanics of Large Bubbles Rising Through Extended Liquids and Through Liquids in Tubes, *Proceeding of Royal Society, A* 200, pp 375-384.
- Kendoush, A.A., (2000), Hydrodynamics and Heat Convection From a Disc Facing a Uniform Flow, Submitted to the *International Journal of Heat and Mass Transfer*.
- Khedher, Ali. K., (2000), Theoretical and Experimental Investigation of Unsteady Forces on a Cascade of Axial Flow Compressor Blades, M.Sc Thesis, College of Engineering, Univ. of Baghdad.
- Michael, P., (1966), Steady Motion of a Disc in a Viscous Fluids. *The Physics of Fluids*, Vol.9, No.2, pp 466-471.
- Roos, W., and Willmarth, W., (1971), Some Experimental Results on Sphere and Disc Drag, *AIAA Journal*, Vol.9, No.2, pp 285-291.
- Ower, E., and Pankhurst, R., (1977), *The Measurement of Airflow*, 5<sup>th</sup> ed. in SI units, Pergamon Press.



**NOMENCLATURE**

Symbol	Description
A	Area of the disc ( $m^2$ )
a	Radius of disc(m)
b	Base of the sting (m)
h	High of the sting (m)
C	Center to center distance between each neighbor pressure holes (m)
$C_p$	Pressure coefficient
$C_D$	Drag coefficient
D	Drag force (N)
d	Diameter of pressure hole (m)
E	Modulus of elasticity ( $N/m^2$ )
F	Force (N)
g	Acceleration. ( $m/s^2$ )
$I_z$	Moment of Inertia about Z-axis ( $m^4$ )
P	Pressure at any point ( $N/m^2$ )
$P_c$	The pressure at center of the disc ( $N/m^2$ )
q	Dynamic pressure ( $N/m^2$ )
Re	Reynolds number( $V2a/v$ )
r	Distance from center of the disc to one pressure hole (cm)
V	Free stream velocity (m/s)
X	Displacement (m)

**GREEK SYMBOLS**

Symbol	Description
$\theta$	Angle of disc inclination from horizontal axis (deg)
$\rho$	Density ( $kg/m^3$ )

**SUBSCRIPTS**

Symbol	Description
o	Stagnation
$\theta$	Refereed to angle position
$A_1, A_2, B_1, B_2$	Position of strain gages locating symmetrically on sting
f	Refereed to front side of disc
R	Refereed to semi vertical

